

Magnetic Switching Dynamics in a Ferrimagnetic Two Sub-Lattice Model including Ultrafast Exchange Scattering

Alexander Baral and Hans Christian Schneider*

Physics Department and Research Center OPTIMAS,
University of Kaiserslautern, 67663 Kaiserslautern, Germany
(Dated: December 7, 2024)

We study the heat-induced magnetization dynamics in a toy model, which includes localized spins antiferromagnetically coupled to an itinerant carrier system with a Stoner gap. We determine the one-particle spin-density matrix including exchange scattering between the localized and itinerant spins as well as scattering with phonons. Depending on the excitation and system parameters we find demagnetization, a transient ferromagnetic-like state, and switching. While a transient ferromagnetic-like state can always be achieved by strong enough excitation, switching occurs only if, in addition, the ferromagnetic coupling between the itinerant carriers is large enough.

PACS numbers: 72.25.Rb, 75.78.-n, 75.78.Jp, 77.80.Fm

I. INTRODUCTION

Heat-induced demagnetization in ferromagnets has been established experimentally for almost twenty years,¹ and has led over this rather long time to several theoretical approaches^{2–9} that capture different aspects of the problem; most notably perhaps the phenomenological 3 temperature model (3TM), which was originally introduced a decade earlier.¹⁰

Compared to this history, heat-induced reversal of magnetization in ferrimagnetic alloys¹¹ is a recent development that has generated a lot of attention because it realizes an ultrafast *deterministic* switching without magnetic fields that may pave the way to a faster magnetic logic. The theoretical understanding of this effect is just being developed using models that in one way or another include (at least) two sub-lattices of localized spins as well as exchange interactions between the different lattices¹² and a coupling to a bath. On the phenomenological side there is the Baryakhtar equation;¹³ more microscopic approaches include atomistic classical spin models coupled to a bath^{14,15} as well as the two-sublattice Landau-Lifshitz-Bloch equation,^{16–19} which implicitly includes a bath average. These approaches have in common, that (i) they are derived from essentially classical models that generate the correct correlation functions *in equilibrium*, (ii) they do not describe delocalized electrons and (iii) the coupling of the localized spin systems to the bath, which may be a phonon or an electron bath depending on the time scale, is not established microscopically. Recently an approach including itinerant carriers⁶ has been used to model two-sublattice systems,²⁰ but this model is based on a non-standard electron-phonon hamiltonian and separates the charge degrees of electrons from their spins so that its spin systems essentially are also two types of localized spins coupled to a bath.

Perhaps the central problems that should be addressed by theoretical models of magnetic switching is how and why a transient ferromagnetic-like state (TFS) occurs in non-equilibrium dynamics of antiferro- or ferrimagnets after excitation by ultrashort pulses, and how a switch-

ing of the magnetization is related to the TFS. These questions have been discussed using the different theoretical approaches cited above, which all entail localized spin systems. Here, we approach this problem in the framework of a microscopic model that is capable of including *all* the relevant interactions of exchange-coupled *localized and delocalized carriers* in a microscopic fashion. Although the model used in this paper, which is inspired by magnetic semiconductors, is too simplified to have predictive power, it is derivable from a Hamiltonian that uses standard expression for carrier-carrier and carrier-phonon interactions. In addition to providing qualitative insights it can, in the future, be systematically improved. The methods of the present paper bear some similarity to those employed by Cywiński and Sham² on ultrafast demagnetization in an *sp-d* model, but their calculations do not reach as far into non-equilibrium regimes as ours do.

II. MODEL

The model used in the following contains (i) dispersionless localized spins \vec{S} and (ii) itinerant carriers with a parabolic dispersion. We will refer to the itinerant carriers also as electrons. For simplicity we assume the electron spin to be $s = 1/2$ and the localized spin $S = 1$, which resembles 3d electrons in iron and localized 4f spins in gadolinium, respectively. Denoting the localized spin states by $|\nu\rangle = \pm 1, 0$ and the electron states by $|\vec{k}\sigma\rangle$, where $\sigma = \pm$, we calculate dynamically the spin-resolved one-particle density matrices of the electrons $\rho_k^{\sigma\sigma'}$ and the localized spins $\rho_{\text{loc}}^{\nu\nu'}$ with an equation of motion technique. Using the spin-dependent reduced density matrices we do not separate the charge and the spin of the itinerant electrons, as done in models that work with three temperatures, most notably with different spin and electron temperatures. “Magnetic” contributions are an antiferromagnetic exchange interaction J between both sub lattices and a Stoner-like on-site cou-

pling U among itinerant carriers. The latter is treated in mean-field approximation and favors a ferromagnetic electron spin polarization. Long and short range (U) contributions to electronic Coulomb scattering are neglected because (i) they do not change the itinerant spin polarization, and (ii) for the conditions studied here, the electronic distributions never deviate much from Fermi-Dirac distributions.²¹ By contrast, we include both mean field and scattering contributions from the exchange interac-

tion between both localized and itinerant spins, as well as a coupling of the itinerant carriers to acoustic phonons at the level of Boltzmann scattering integrals. Throughout, we work with single-particle states that are obtained from a diagonalization including the exchange and Stoner mean-field contributions. The resulting mean-field energies are denoted by E_ν for the localized spins and $\epsilon_{\vec{k}\sigma}$ for the spin-split electron bands. The relevant equations of motion then take the following form

$$\frac{\partial}{\partial t} \rho_{\text{loc}}^{\nu\nu'} = \frac{i}{\hbar} (E_\nu - E_{\nu'}) \rho_{\text{loc}}^{\nu\nu'} + \frac{\partial}{\partial t} \rho_{\text{loc}}^{\nu\nu'} \Big|_{\text{xc}} \quad (1)$$

$$\frac{\partial}{\partial t} \rho_{\vec{k}}^{\sigma\sigma'} = \frac{i}{\hbar} (\epsilon_{\vec{k}\sigma} - \epsilon_{\vec{k}\sigma'}) \rho_{\vec{k}}^{\sigma\sigma'} + \frac{\partial}{\partial t} \rho_{\vec{k}}^{\sigma\sigma'} \Big|_{\text{xc}} + \frac{\partial}{\partial t} \rho_{\vec{k}}^{\sigma\sigma'} \Big|_{\text{e-pn}} - \frac{\rho_{\vec{k}}^{\sigma\sigma'} - \delta_{\sigma\sigma'} F_{\vec{k}}^\sigma}{\tau_{\text{sf}}} \quad (2)$$

The first terms in Eq. (1) and (2) are coherent contributions, which describe precessional motion of one spin around the mean-field of the spin of the other species. All the other terms are incoherent terms. The incoherent exchange scattering contributions at the level of Boltzmann scattering integrals are given by

$$\begin{aligned} \frac{\partial}{\partial t} \rho_{\text{loc}}^{\nu_1\nu_2} \Big|_{\text{xc}} &= \frac{i}{\hbar} \sum_{\vec{k}\vec{k}'} \sum_{\sigma_1 \dots \sigma_4} \sum_{\nu_3\nu_4\nu_5} W_{\vec{k}'\sigma_1\vec{k}\sigma_2}^{\nu_5\nu_1} (W_{\vec{k}'\sigma_3\vec{k}\sigma_4}^{\nu_3\nu_4})^* \\ &\cdot \frac{\delta_{\nu_4\nu_2} \rho_{\text{loc}}^{\nu_5\nu_3} \rho_{\vec{k}'}^{\sigma_1\sigma_3} (\delta_{\sigma_4\sigma_2} - \rho_{\vec{k}}^{\sigma_4\sigma_2}) - \delta_{\nu_5\nu_3} \rho_{\text{loc}}^{\nu_4\nu_2} \rho_{\vec{k}}^{\sigma_4\sigma_2} (\delta_{\sigma_1\sigma_3} - \rho_{\vec{k}'}^{\sigma_1\sigma_3})}{\epsilon_{\vec{k}\sigma_4} - \epsilon_{\vec{k}'\sigma_3} + E_{\nu_4} - E_{\nu_3} - i\gamma} + (\nu_1 \leftrightarrow \nu_2)^* \end{aligned} \quad (3)$$

and

$$\begin{aligned} \frac{\partial}{\partial t} \rho_{\vec{k}}^{\sigma_1\sigma_2} \Big|_{\text{xc}} &= \frac{i}{\hbar} \sum_{\vec{k}'} \sum_{\nu_1\nu_2\nu_3\nu_4} \sum_{\sigma_3\sigma_4\sigma_5} W_{\vec{k}'\sigma_5\vec{k}\sigma_1}^{\nu_1\nu_2} (W_{\vec{k}'\sigma_3\vec{k}\sigma_4}^{\nu_3\nu_4})^* \\ &\cdot \frac{\delta_{\nu_4\nu_2} \rho_{\text{loc}}^{\nu_1\nu_3} \rho_{\vec{k}'}^{\sigma_5\sigma_3} (\delta_{\sigma_4\sigma_2} - \rho_{\vec{k}}^{\sigma_4\sigma_2}) - \delta_{\nu_1\nu_3} \rho_{\text{loc}}^{\nu_4\nu_2} \rho_{\vec{k}}^{\sigma_4\sigma_2} (\delta_{\sigma_3\sigma_5} - \rho_{\vec{k}'}^{\sigma_3\sigma_5})}{\epsilon_{\vec{k}\sigma_4} - \epsilon_{\vec{k}'\sigma_3} + E_{\nu_4} - E_{\nu_3} - i\gamma} + (\sigma_1 \leftrightarrow \sigma_2)^* \end{aligned} \quad (4)$$

Here, γ denotes an infinitesimal broadening and we use the abbreviation

$$W_{\vec{k}\sigma\vec{k}'\sigma'}^{\nu\nu'} \equiv J \langle \vec{k}\sigma | \hat{\vec{S}} | \vec{k}'\sigma' \rangle \langle \nu | \hat{\vec{S}} | \nu' \rangle \quad (5)$$

where $\hat{\vec{S}}$ and $\hat{\vec{S}}$ are the spin-operators of the localized and the itinerant electrons. The electron-phonon scattering (e-pn) contribution in Eq. (2) is a standard expression, an explicit derivation of which with special attention to spin splitting is given in Ref. 22. It is an important property of scattering with long-wavelength longitudinal phonons that it does *not* lead to a transfer of angular momentum from the itinerant carriers to the lattice, it only cools down the itinerant carrier system and increases the temperature of the phonon system in accordance with energy conservation. The transfer of angular momentum to the lattice is left to a relaxation-time expression in Eq. (2) because the fundamental mechanism is not the important point of this paper. Likely it is a combination of electron-phonon/electron-electron scattering and spin-orbit coupling.^{5,21} We generally assume spin-

flip processes to be faster than the heat transfer to the phonons, but slower than the exchange scattering. In Eq. (4), $F_{\vec{k}}^\sigma = f(\epsilon_{\vec{k}\sigma} - \mu_F)$ denotes a Fermi-Dirac distribution with the same energy as the actual $\rho_{\vec{k}}^{\sigma\sigma'}$, but equal chemical potentials μ_F for both spins.

We determine the equilibrium configuration self-consistently, assuming that the equilibrium reduced density matrix

$$\rho_{\vec{k}}^{\sigma\sigma'} = \delta_{\sigma,\sigma'} f(\epsilon_{\sigma\vec{k}} - \mu_0) \quad (6)$$

is spin diagonal and given by Fermi-Dirac distributions with temperature T_0 and equal chemical potentials μ_0 for both spin states. The average spins \vec{S} and \vec{s} of the two species are parallel to the mutual exchange field. Depending on the value of the coupling constants J and U the itinerant system is either partially or fully spin polarized. In the numerical calculations below, as done in Ref. 22, we employ two-dimensional \vec{k} vectors because it reduces the numerical complexity of propagating the

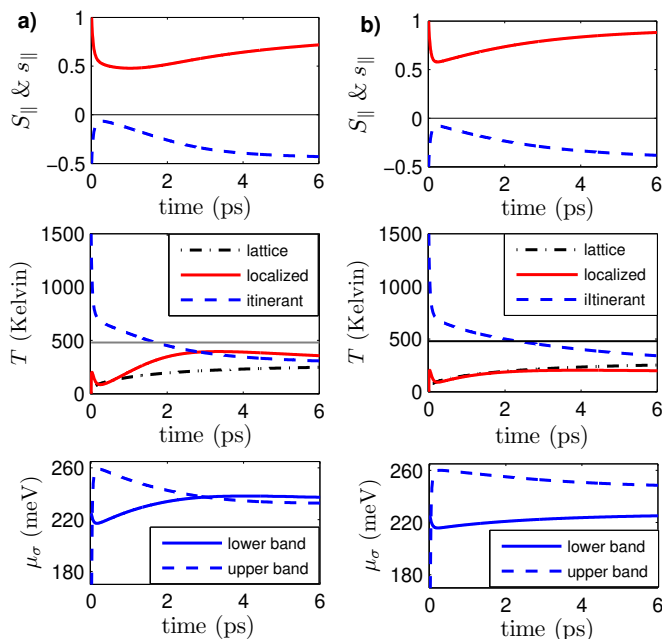


FIG. 1. Computed results for demagnetization scenario with $J = 100$ meV, $U = 400$ meV, and $T_e^{(0)} = 1500$ K. The spin-flip times are $\tau_{sf} = 200$ fs (a) and $\tau_{sf} \rightarrow \infty$ (b). Top: Dynamics of the averaged localized spin S_{\parallel} (solid curve) and itinerant spin s_{\parallel} (dashed curve); middle: quasi-equilibrium temperatures and T_C (thin line); bottom: quasi-chemical potentials for the two itinerant bands.

scattering calculations over long times. This simplification also changes the equilibrium spin polarization, exchange splitting and the Curie temperature compared to three-dimensional \vec{k} vectors. In the following numerical calculations we always assume a common initial temperature of all three sub-system $T_0 = 10$ K, which is far lower than the Curie temperature T_C .

We model the excitation of a short linearly-polarized laser pulse as an instantaneous heating of the itinerant carriers at $t = 0$. We assume that the localized spin system is not excited optically.⁹ Immediately after the excitation the itinerant spin density-matrix $\rho_{\vec{k}}^{\sigma\sigma'}$ is assumed to be spin diagonal with the spin dependent distributions determined by Fermi functions with the same spin-expectation value but with an elevated initial temperature $T_e^{(0)}$ that usually exceeds T_C . Even though the spin polarization of the carriers does not change, the chemical potentials μ_{σ} become different.

III. RESULTS

Figure 1 presents the key dynamical quantities for an excitation characterized by $T_e^{(0)} = 1500$ K as well as a short and infinitely long spin-flip time, respectively. The parameters $J = 100$ meV and $U = 400$ meV give rise to a Curie temperature of $T_C = 480$ K. These parameters

together with the initial carrier temperature $T_e^{(0)}$ lead to a demagnetization scenario, regardless of the spin-flip time τ_{sf} , as shown in the top panel. The components of both localized and itinerant spins parallel to the mutual exchange field, S_{\parallel} and s_{\parallel} , show an *ultrafast* symmetric decrease due to exchange scattering on a timescale of several ten femtoseconds. The exchange scattering conserves the total angular momentum and energy of the combined system of spin-split itinerant carriers and localized spins, so that such an ultrafast drop does not occur for a ferromagnetic exchange coupling.¹³ We have checked this also for our model. We will analyze the ultrafast dynamics due to the exchange scattering in more detail below.

Compared to the intrinsic time scale of the exchange scattering, spin-flip scattering, which dissipates only carrier angular momentum, and carrier-phonon scattering, which only transfers heat from the itinerant carriers to the phonon system, act on much longer time scales of hundreds of fs and several ps, respectively. During the comparatively slow remagnetization process, the angular momentum and energy transfer between the localized and itinerant sub-systems due to the exchange scattering is limited to the times scales of these slower mechanisms. Changing the spin-flip scattering time in Fig. 1(b) as compared to (a) does not change the qualitative behavior.

In the middle panel of Fig. 1 we show the quasi-equilibrium temperatures of the itinerant carriers (or “electrons”) T_e , the localized spins T_{loc} and the phonons T_L , which are obtained from the computed dynamics of the spin density matrix as the temperatures of thermalized distributions with the same energy as the non-equilibrium distributions. Note, in particular, that the excited electrons have a quasi-equilibrium temperature $T_e(t)$ and *different* chemical potentials $\mu_{\sigma}(t)$ for each spin species, as shown in the bottom panel of Fig. 1. With a non-vanishing spin-flip rate τ_{sf}^{-1} as in Fig. 1(a), the temperatures of the itinerant electrons T_e and of the localized spins T_{loc} essentially converge on the time scale of the spin-flip relaxation τ_{sf} . The phonon temperature T_L approaches these two on the time scale of the electron-phonon scattering. Figure 1(b) shows that without dissipation of angular momentum, viz. $\tau_{sf} \rightarrow \infty$, T_{loc} does not get close to T_e . This makes clear that exchange scattering neither simply equalizes the temperatures T_{loc} and T_e , nor the chemical potentials μ_{σ} .

We next model stronger excitations by raising $T_e^{(0)}$ in Fig. 2. The parameter U in Fig. 2 (a) is the same as before so that we have $T_C \simeq 480$ K. In addition, we relax the lattice temperature toward T_0 with a time constant of 10 ps to include the effect of heat diffusion. This guarantees a final remagnetization without affecting the faster dynamics. For Fig. 2(b) we increase U to 500 meV, which leads to $T_C \simeq 1200$ K. For the same material parameters as in Fig. 1(a), Fig. 2 exhibits a TFS starting around 50 fs and persisting up to about 2 ps. During the TFS, the localized spins experience a population inversion and the corresponding spin-temperature T_{loc} is no longer well de-

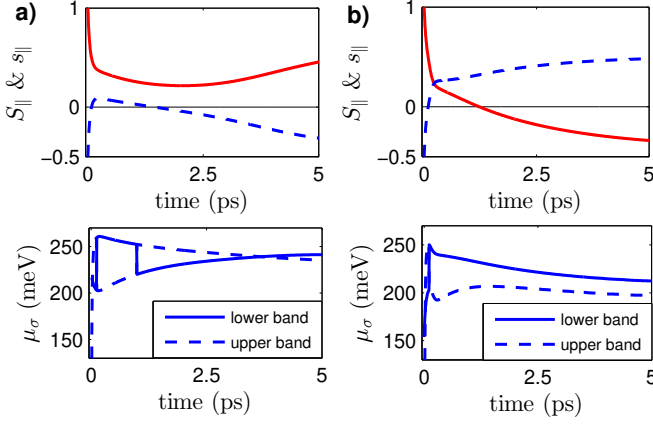


FIG. 2. Top: Computed dynamics of the average localized spin S_{\parallel} (solid curve) and the average itinerant spin s_{\parallel} (dashed curve) for a TFS scenario with $T_e^{(0)} = 2000$ K and $U = 400$ meV (a) as well as a switching scenario with $T_e^{(0)} = 2500$ K and $U = 500$ meV (b). Bottom: Electronic quasi-chemical potentials. $J = 100$ meV is unchanged.

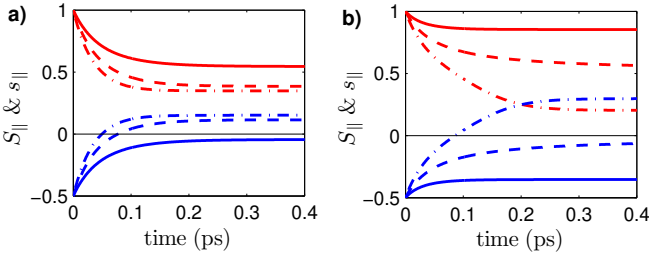


FIG. 3. Computed dynamics of average localized spin S_{\parallel} (red, starting from 1) and average itinerant spin (blue, starting from -0.5) after excitation with $T_e^{(0)} = 1500$ K (solid lines), $T_e^{(0)} = 2000$ K (dashed lines) and $T_e^{(0)} = 2500$ K (dashed-dotted lines) for $U = 400$ meV (a), $U = 500$ meV (b), and $J = 100$ meV.

finer. As the coupling to the phonons cools down the itinerant carriers, the system either returns, as in Fig. 2(a), into its initial state or, as in Fig. 2(b), remagnetizes with an inverse orientation and thus undergoes magnetization switching (SW). Note that in Fig. 2(b) the itinerant carriers become fully spin-polarized, $s_{\parallel} \simeq 1/2$, around 2.5 ps so that the exchange scattering cannot further remagnetize the localized spins. Note that we label the eigenstates according to their energy, so that this label changes if the effective mean-field splitting changes its sign. Comparing the bottom panels of Figs. 1 and 2 indicates that the difference between the chemical potentials does not drive the switching or demagnetization dynamics.

In Fig. 3 we come back to the role of the exchange scattering in realizing the TFS. We plot here for different initial temperatures $T_e^{(0)}$ the computed dynamics obtained by including only exchange scattering. While this leads to an unphysical steady state, it illustrates the way in

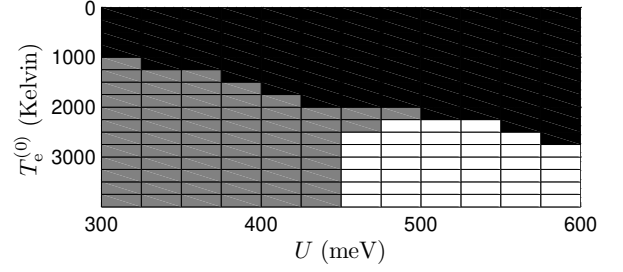


FIG. 4. Color-coded dynamics: demagnetization (black), transient ferromagnetic-like state (grey) and switching (white) as a function of Stoner parameter U and excitation temperature $T_e^{(0)}$. The exchange coupling constant is $J = 100$ meV.

which exchange scattering works. In Fig. 3(a), for $U = 400$ meV, an initial itinerant temperature $T_e^{(0)} = 1500$ K leads to a state with reduced localized spin, i.e., demagnetization in each spin system. Increasing $T_e^{(0)}$ leads to a reversal of the itinerant spin s_{\parallel} and thus a TFS on the timescale of the exchange scattering. This behavior occurs because the exchange scattering redistributes the deposited energy as well as angular momentum between the itinerant and localized spins all the while satisfying both conservation of total energy and total angular momentum. In Fig. 3(b) the Stoner parameter is increased to $U = 500$ meV, which is indicative of a more rigid itinerant carrier magnetism. Correspondingly, for the smaller initial temperatures $T_e^{(0)}$ the demagnetization of each spin system due to exchange scattering is reduced compared to Fig. 3(a). However, for the highest excitation, i.e., $T_e^{(0)} = 2500$ K not only a TFS occurs, but the average itinerant spin s_{\parallel} becomes larger than the average localized spin S_{\parallel} . Thus the redistribution of the deposited energy during the ultrafast exchange scattering obviously is decisive for the following behavior. However, the excitation condition alone does not determine whether switching occurs, because the dynamics of the mean-field gaps obviously play an important role and the Stoner coupling has to stabilize the itinerant spin to achieve $s_{\parallel} > S_{\parallel}$. If this rather violent change of the different average spins occurs during the ultrafast dynamics, it cannot be undone by the “gentler” dynamics on longer timescales, which has been discussed in connection with Fig. 1. From this intermediate reversed state $s_{\parallel} > S_{\parallel}$, slower mechanisms cause the spins to relax toward their equilibrium length but with reversed orientation.

In Fig. 4 we collect the results from individual calculations as shown in Fig. 1(a) and 2 by plotting the type of dynamics: demagnetization, transient ferromagnetic-like state (TFS) and switching vs. excitation temperature $T_e^{(0)}$ and the strength of the itinerant ferromagnetic coupling constant U in the carrier system. We find that there is a threshold for the temperature $T_e^{(0)}$, below which the system only de- and remagnetizes into its initial orienta-

tion (without entering a TFS). It depends on the Stoner parameter U whether, for high enough $T_e^{(0)}$, “only” a TFS occurs or whether heat-induced switching can be achieved. The results of these model calculations make it likely that materials with a stronger ferromagnetic coupling in the itinerant carrier system, which is determined by the Stoner parameter U in the present paper, are better suited to achieve heat-induced magnetic switching.

IV. CONCLUSION

In conclusion, we investigated magnetic dynamics in a two-sublattice model that contains both localized spins and itinerant electrons, which are antiferromagnetically

coupled by an exchange interaction. In addition, the itinerant carriers experience a mean-field (Stoner) spin splitting. We calculated the spin dependent dynamics under the influence of the ultrafast exchange scattering as well as electron-phonon scattering with a phonon bath. We found different types of dynamics: demagnetization (of each spin system), a transient ferromagnetic-like state, as well as magnetic switching. The dynamics depends on the initial energy deposited in the itinerant electron system as well as the coupling constants. It is found that the ferromagnetic coupling has to be strong enough to allow the initial ultrafast exchange scattering dynamics to drive a “sufficiently ferromagnetic” transient state, which can then evolve on a slower timescale to a switched magnetization state.

-
- * hcsch@physik.uni-kl.de
- ¹ E. Beaurepaire, J.-C. Merle, A. Daunois, and J.-Y. Bigot, *Physical Review Letters* **76**, 4250 (1996).
 - ² L. Cywiński and L. J. Sham, *Physical Review B* **76**, 045205 (2007).
 - ³ U. Atxitia, O. Chubykalo-Fesenko, N. Kazantseva, D. Hinzke, U. Nowak, and R. W. Chantrell, *Applied Physics Letters* **91**, 232507 (2007).
 - ⁴ D. Steiauf and M. Fähnle, *Physical Review B* **79**, 140401 (2009).
 - ⁵ M. Krauß, T. Roth, S. Alebrand, D. Steil, M. Cinchetti, M. Aeschlimann, and H. Schneider, *Physical Review B* **80** (2009).
 - ⁶ B. Koopmans, G. Malinowski, F. Dalla Longa, D. Steiauf, M. Fähnle, T. Roth, M. Cinchetti, and M. Aeschlimann, *Nature materials* **9**, 259 (2010).
 - ⁷ S. Essert and H. C. Schneider, *Physical Review B* **84**, 224405 (2011).
 - ⁸ U. Atxitia and O. Chubykalo-Fesenko, *Physical Review B* **84**, 144414 (2011).
 - ⁹ A. Manchon, Q. Li, L. Xu, and S. Zhang, *Physical Review B* **85**, 064408 (2012).
 - ¹⁰ M. B. Agranat, S. I. Ashikov, A. B. Granovskii, and G. I. Rukman, *Zh. Eksp. Teor. Fiz* **86**, 1376 (1986).
 - ¹¹ I. Radu, K. Vahaplar, C. Stamm, T. Kachel, N. Pontius, H. A. Dürr, T. A. Ostler, J. Barker, R. F. Evans, R. W. Chantrell, *et al.*, *Nature* **472**, 205 (2011).
 - ¹² N. Bergeard, V. López-Flores, V. Halté, M. Hehn, C. Stamm, N. Pontius, E. Beaurepaire, and C. Boeglin, *Nature communications* **5** (2014).
 - ¹³ J. H. Mentink, J. Hellsvik, D. V. Afanasiev, B. A. Ivanov, A. Kirilyuk, A. V. Kimel, O. Eriksson, M. I. Katsnelson, and T. Rasing, *Physical Review Letters* **108**, 057202 (2012).
 - ¹⁴ S. Wienholdt, D. Hinzke, K. Carva, P. M. Oppeneer, and U. Nowak, *Physical Review B* **88**, 020406 (2013).
 - ¹⁵ T. A. Ostler, J. Barker, R. F. Evans, R. W. Chantrell, U. Atxitia, O. Chubykalo-Fesenko, S. El Moussaoui, L. Le Guyader, E. Mengotti, L. J. Heyderman, *et al.*, *Nature communications* **3**, 666 (2012).
 - ¹⁶ U. Atxitia, T. Ostler, J. Barker, R. F. Evans, R. W. Chantrell, and O. Chubykalo-Fesenko, *Physical Review B* **87**, 224417 (2013).
 - ¹⁷ D. A. Garanin, *Physical Review B* **55**, 3050 (1997).
 - ¹⁸ H. Kronmüller and S. Parkin, eds., *Handbook of Magnetism and Advanced Magnetic Materials* (John Wiley & Sons, Ltd, Chichester, UK, 2007).
 - ¹⁹ N. Kazantseva, D. Hinzke, U. Nowak, R. Chantrell, U. Atxitia, and O. Chubykalo-Fesenko, *Physical Review B* **77** (2008).
 - ²⁰ A. J. Schellekens and B. Koopmans, *Physical Review B* **87**, 020407 (2013).
 - ²¹ B. Y. Mueller, A. Baral, S. Vollmar, M. Cinchetti, M. Aeschlimann, H. C. Schneider, and B. Rethfeld, *Physical Review Letters* **111**, 167204 (2013).
 - ²² A. Baral, S. Vollmar, and H. C. Schneider, *Physical Review B* **90**, 014427 (2014).